Макрогетероциклы

http://mhc-isuct.ru

Coordination Reaction of Poly-4-vinylpyridine by Cobalt Porphyrinate in Nanostructured Layers at the Air-Water Interface

L. A. Maiorova,[a,b@] M. V. Petrova,[a] T. A. Ageeva,[a] and A. N. Gromov[b]

[a]Ivanovo State University of Chemistry and Technology, 153000 Ivanovo, Russia
[b]Federal Research Center "Computer Science and Control" of RAS, 119333 Moscow, Russia
[@]Corresponding author E-mail: maiorova.larissa@gmail.com

We dedicate this work to the memory of Oskar Koifman, who contributed much
to the study of Langmuir-Blodgett films and nanomaterials, passed on his experience
to the next generations of researchers, and made this study possible

Nanostructured layers of poly-4-vinylpyridine (P4VP) are formed at air-water interfaces. Quantitative characteristics of their structure and properties are analyzed within the framework of the model of nanostructured M-monolayer. For the first time, the coordination reaction of poly-4-vinylpyridine with cobalt tetra(p-methoxyphenyl)porphyrinate (CoTpMPP) was carried out in nanostructured layers at the air-water interface. The resulting Langmuir-Schaefer films of P4VP-CoTpMPP were studied by UV-Vis spectroscopy.

Keywords: Nanostructured layers, air-water interface, coordination reaction, Langmuir-Schaefer films, poly-4-vinylpyridine, cobalt porphyrinate.

Реакция координации поли-4-винилпиридина порфиринатом кобальта в наноструктурированных слоях на границе раздела вода-воздух

Л. А. Майорова,[a,b@] М. В. Петрова,[a] Т. А. Агеева,[a] А. Н. Громов[b]

[a]Ивановский государственный химико-технологический университет, 153000 Иваново, Россия
[b]Федеральный исследовательский центр «Информатика и управление» РАН, 119333 Москва, Россия
[@]E-mail: maiorova.larissa@gmail.com

На границе раздела вода-воздух сформированы наноструктурированные слои поли-4-винилпиридина (П4ВП). Количественные характеристики их структуры и свойств проанализированы в рамках модели наноструктурированного М-монослоя. Впервые реакция координации поли-4-винилпиридина тетра(пара-метоксифенил)порфиринатом кобальта (СоТрМРР) проведена в наноструктурированных слоях на границе раздела вода-воздух. Полученные пленки Ленгмюра-Шефера П4ВП-СоТрМРР исследованы методом электронной спектроскопии поглощения.

Ключевые слова: Наноструктурированные слои, граница раздела вода-воздух, реакция координации, пленки Ленгмюра-Шефера, поли-4-винилпиридин, порфиринат кобальта.

Introduction

Materials based on macroheterocycles have found numerous applications as catalysts,[1,2] sensors,[3] components of organic electronic devices,[4] and others.

Porphyrins and their metal complexes exhibit excellent stability in solutions and thin films. Metalloporphyrins play a crucial role in organizing and carrying out photosynthetic, respiratory, enzymatic, and other functions in living organisms.[5-7] With their unique set of properties, they are

capable of forming supramolecular complexes with proteins and other biomolecules. Therefore, interest in self-organizing structures based on metalloporphyrins, of both natural origin and their models, continues to grow.[8] Methods for fixing porphyrins on the surface include Langmuir-Blodgett method,[9-11] encapsulation,[12-16] sublimation in a vacuum, adsorption of porphyrins from solutions, impregnation of a solid carrier with subsequent removal of the solvent, mechanical grinding of porphyrins with a carrier (in particular, with a polymer), *etc*.[17-19] Spontaneous assembly of the most complex spatial structures based on metalloporphyrins in biological media involves all types of binding: covalent, ionic, coordination, each of which is responsible for a specific fragment of the tetrapyrrole complex.

Compounds of this class tend to form supramolecular structures (so-called stacks). Thin films of porphyrins can be prepared by a variety of methods, including vacuum sublimation, electrochemical deposition, solution casting, and the Langmuir-Blodgett method. Using the Langmuir-Blodgett technology, it is possible to form films with a given structure and thickness in the nanometer range.[20-23]

Nowadays, nanostructures of numerous biomolecules having different properties from those of the parent molecules and with great potential for various applications have been reported.[24-26] The formation of different kinds of supramolecular assemblies from precursor compounds at the water surface,[27-30] during electrochemical deposition on electrodes,[31,32] and in metal-organic frameworks[33,34] has been reported. Self-assembly plays an essential role in materials nanoarchitectonics.[35-43] Supramolecular polymers have been created using diverse self-assembly strategies wherein biomolecules[44-47] are employed.[48] Previously, we have demonstrated the possibility of supramolecular design at the air-water interface by controlling the self-assembly of tetrapyrrole compounds into 2D and 3D nanostructures. The concept of nanostructuring of organic compounds at the air-water interface and a model of a floating layer, the structural units of which can be both individual molecules (Langmuir's approach, special case) and their major nanostructures (so-called M-nanostructures, general case), were presented.[49-53] The formation of the porphyrin supermolecules from magnesium porphine, a functional element of chlorophyll, was reported.[49] Recently, we have reported the formation of the first supermolecular nanoentities (SMEs) of a vitamin B$_{12}$ derivative (monocyano-species of heptabutyl cobyrinate), unique nanoparticles with strong noncovalent intermolecular interactions, and emerging optical and redox properties.[53] Nanostructured thin films based on tetrapyrroles have been extensively studied in sensor systems. Sensor responses have been explained by the complexation of analytes with Co(II) ion of tetrapyrroles.[54-58]

The incorporation of metalloporphyrin into a polymer matrix using copolymerization or polymer-analogous transformation methods makes it possible to obtain a group of polymeric materials called porphyrin polymers.[59] Interest in the production of porphyrin polymers is due to the possibility of formation from them of functional thin films in which porphyrin is not aggregated. Currently, porphyrin polymers are used as sensors, catalysts for various processes, gas separation membranes, medications, sensi

tizers for photodynamic therapy, *etc*.[60-63] Polymer nanosponges of various natures were proven to be promising as not only "nanoreactors" and "nanocatalysts," but also as unique systems for targeted drug delivery.[64] As shown in[65], polymer micelles based on polyethylene glycol-block-poly-4-vinylpyridine (PEG-b-P4VP), obtained through axial coordination, increase the water solubility and photostability of hydrophobic Zn, Mg tetraphenylporphyrin. P4VP with Spiro-OMeTAD is used as a basis for the preparation of perovskite solar cells and other optoelectronic devices.[66] Poly-4-vinylpyridine is also used as a cheap, effective and recyclable catalyst.[67,68]

The synthesis of porphyrin polymer materials is most often carried out in solutions or powders. The possibility of obtaining porphyrin polymers in nanostructured layers at the water-air interface is an interesting problem both from the point of view of studying the fundamental processes of self-organization of organic compounds and for practical applications.

In this work, we have studied the possibility of forming nanostructured layers of poly-4-vinylpyridine on the surface of water, carrying out the coordination reaction of poly-4-vinylpyridine (P4VP) with cobalt tetra(*p*-methoxyphenyl)porphyrinate (CoTpMPP) and obtaining the porphyrin polymer P4VP-CoTpMPP at the water interface - air and in LS films on solid substrates.

Experimental

To calculate the initial degrees of coverage of the water surface with molecules and analyze the obtained experimental data, a model of a unit of a poly-4-vinylpyridine molecule (Figure 1a) and a fragment of the closest packing of polymer chains (Figure 1b) was built. For calculations, we used the HyperChem 8.0.8 software package (PM3 calculation method).

Geometric parameters of the molecule link: 0.8×0.5 nm, projection area – $A_{proj} = 0.27$ nm^2, area of the circumscribed rectangle – $A_{rec} = 0.4$ nm^2. The minimum area per link in the package is 0.2 nm^2.
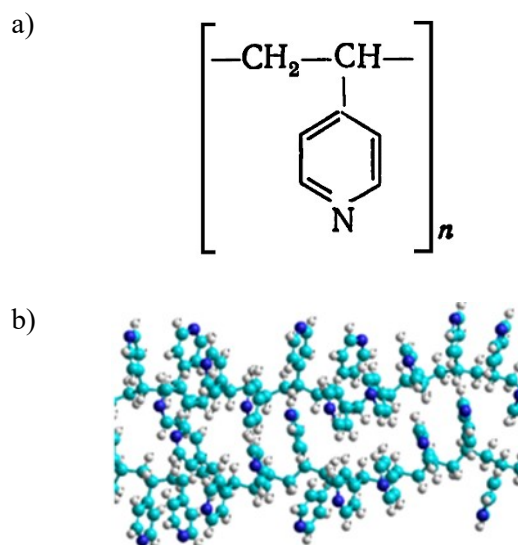
a)

b)

Figure 1. (a) Structural formula, (b) fragment of the packing of P4VP polymer chains.
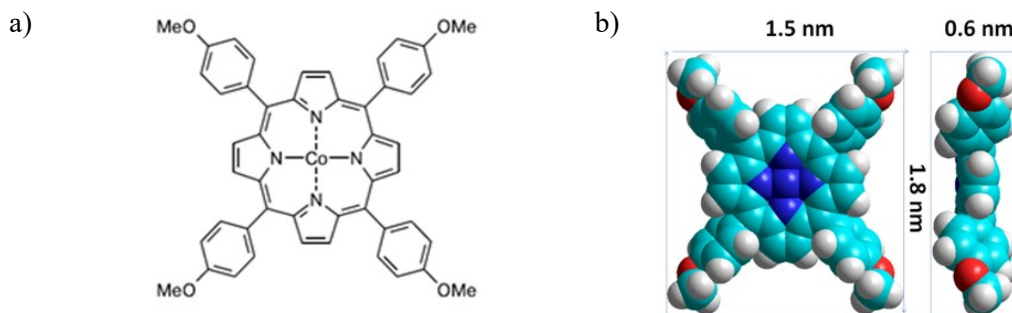
Figure 2. Structural formula (a) and molecule model (b) of cobalt tetra(*p*-methoxyphenyl)porphyrinate (CoTpMPP).
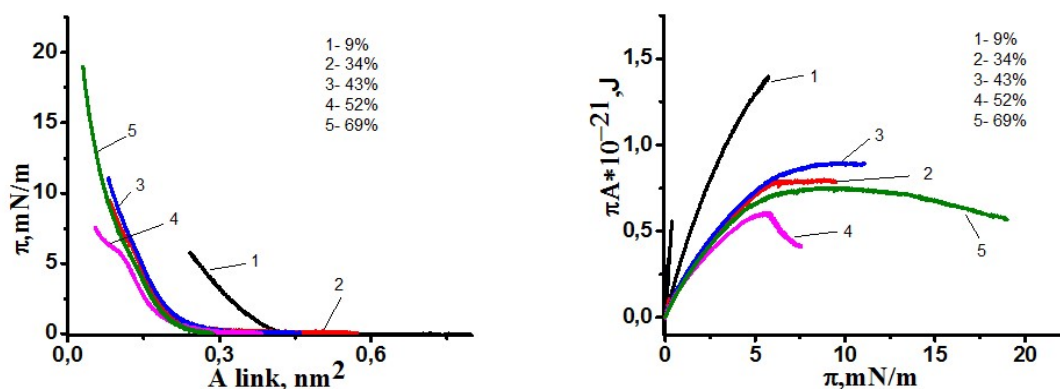

Figure 3. (a) π-A and (b) πA-π Isotherms of P4VP obtained from a solution in chloroform (C=4.12·10^{-6} M), at a layer compression rate of 2.78 cm^2/min. The numbers indicate the current degree of surface coverage before the layer begins to compress (cj-0) in percent.

The structural formula and model of the cobalt tetra(*p*-methoxyphenyl)porphyrinate molecule are presented in Figure 2.

Geometric characteristics of the molecule: 1.8×1.5×0.6 nm, projection areas A_{proj}(face)=1.72 nm^2 and A_{proj}(edge)=0.54 nm^2, areas of circumscribed rectangles A_{rec}(face)=2.7 nm^2 and A_{rec}(edge)=1.1 nm^2, areas in a monolayer with the closest packing, A_{pack}(face)=2.5 nm^2 and A_{pack}(edge)=1.1 nm^2.

To obtain floating layers at the air-water interface, a solution of the compounds under study in chloroform was applied to double-distilled water with a microliter syringe (100 μL, Hamilton, Sweden) at (20±1)°C. The volume required to apply the solution was determined by the required initial degree of coverage of the water surface with a compound. The layers were compressed at a rate of 2.3 cm^2·min^{-1} during 15 minutes after applying the solution to the water surface. The experiments were carried out on the NT-MDT LB trough (Zelenograd, Russia). Surface pressure was measured using a Wilhelmy balance (with an accuracy of 0.02 mN/m).

Langmuir-Schaefer (LS) films were obtained on quartz substrates at (20±1) ºC. The barriers compressing the layer on the water surface were stopped at selected pressure values, after which the layers were successively transferred to the substrate using the horizontal lift method. Electronic absorption spectra of the LS films and solution were recorded on a Shimadzu-UV 1800 spectrophotometer (measurement error at wavelength ±1 nm).

Analysis of the structure of layers at the water-air interface was carried out within the framework of a model and a quantitative method for analyzing compression isotherms of a nanostructured M-monolayer, based on the concept of the layer as a real two-dimensional gas with structural elements representing two-dimensional nanostructures with a diameter of 5–30 nm (M-nanostructures).[49] The stable state of the layer is described by the equation $\pi(A-A_{mol})=kT/n$,[29,38,49] where π is the surface pressure, A is the area per molecule in the layer, A_{mol} is the area per molecule in nanostructures, n is the number of molecules in the nano-structure, k – Boltzmann constant, T – absolute temperature. The compression isotherms of the layer on the water surface, plotted in the πA–π axes, have both linear (corresponding to single-phase states of the layer) and nonlinear sections. The values of A_{mol} and n are the main characteristics of a floating monolayer and can be determined by approximating a section of the πA–π graph with a linear function (the least squares method is used, the πA error does not exceed 3%). The area per molecule in a nanostructure is defined as the tangent of the slope of the straight line, the segment of which approximates the linear section of the graph. The number of molecules is determined by the formula $n=kT/\beta$, where β is the ordinate of the point of intersection of the straight line with the ordinate axis. According to the model used, M-nanostructures have the shape of a circle, the area of which is calculated by the formula $S_{NS}=nA_{mol}$, and the diameter $D_{NS}=2(S_{NS}/\pi)1/2$. The compressibility of the layer in a stable state is defined as $B=(1-A_f/A_i)/(\pi_f-\pi_i)$, where π_i, π_f are the pressures at the beginning and end of the stable state, A_i, A_f are the abscissas of the beginning and end of the linear section π–A isotherms, respectively. The distance between the boundaries of nanostructures is calculated by the formula: $d_i=2(n/\pi)1/2$ ($A_i1/2-A_{mol}1/2$). Water content between nanostructures (at the initial point of the stable state) $w_{inter-M-i}=A_i-A_{mol}$. The following were also calculated: the current degrees of surface coverage at the points of the beginning and end of the stable state – $c_i=A_{proj}/A_i$ and $c_f=A_{proj}/A_f$; pressure range in which a stable state exists $\Delta\pi=\pi_i-\pi_f$.

The error in determining the area per molecule in layer (A) is 2%. The maximum error values of the determined characteristics of the layer are: for A_{mol}, $\Delta\pi$, c_i, c_f – 3%; for c_{j-0} – 5%; for S_{NS} – 6%; for D_{NS} and $w_{inter-M-i}$ – 7%; for B, n, and d_i – 10%.

Results and Discussion

Preparation of nanostructured monolayers of P4VP at the air-water interface

The studies were carried out using a solution of P4VP in chloroform (C=4.12·10⁻⁶ M, MW=60000, MW=105 g/mol, number of units in a polymer molecule=571). Figure 3 shows the π-A and πA-π isotherms of P4VP obtained at a layer compression rate of 2.78 cm²/min. The main results of the analysis of compression isotherms and characteristics of P4VP layers are presented in Table 1. Based on the analysis of the results obtained, it was established that at initial degrees of surface coverage c_{j-0} = 9% in the region of low surface pressures (up to 0.5 mN/m) P4VP monolayers with an area per molecule link in a nanostructure – $A_{mol(link)}$=0.41 nm² (which corresponds to a sparse monolayer with molecules located along the water surface).

The main characteristics of M-monolayers are determined (the size of nanostructures formed in the layer, the number of molecules in them, the distances between them, the water/solvent content between M-aggregates at the initial point of the stable state, the compressibility of the layer).

The data obtained make it possible to construct a model of condensed monolayer. The dependences of the main monolayer parameters $A_{mol(link)}$, n and D_{NS} on the current degree of surface coverage before the start of layer compression (c_{j-0}, Figure 4) were established. Analysis of the dependences of the layer characteristics on the current degree of surface coverage gives the following Equations:

$$A_{mol(link)}=0.39-0.02 \cdot c_{j-0} \tag{1}$$
$$n=const \tag{2}$$
$$D_{NS}=42-0.2 \cdot c_{j-0} \tag{3}$$

These dependencies make it possible to establish constants that do not depend on the conditions of layer formation. The maximum degree of surface coverage at which a monolayer can be formed has been determined. The minimum area per molecule in the layer calculated from the model is 0.2 nm². Therefore, the boundary of the

Table 1. Characteristics of P4VP monolayers at the water-air interface at various current degrees of surface coverage (c_{j-0}).

c_{j-0}, %	Type of nanostructures	π_i–π_f, ($\Delta\pi$) mN/m	$A_{mol(link)}$**, nm²	n_{mol} (n_{link})	c_i^* – c_f^*, %	D_{NS}, nm (S_{NS}, nm²)	$w_{inter-M-i}$, nm²	d_i, nm	B, m/N
9	M-rar	0.02–0.48 (0.46)	0.41	6 (3673)	45–51	44 (1506)	0.03	1.7	227
35		0.08–0,26 (0.18)	0.32	6 (3285)	59–62	37 (1051)	0.02	1.1	312
43	M-cond	0 08–0 26 (0.18)	0.3	5 (2907)	62–66	33 (872)	0.02	1.5	336
52		0.08–0.2 (0.12)	0.28	5 (2886)	66–70	32 (808)	0.03	1.5	332
69		0.02–0.41 (0.40)	0.25	5 (2993)	71–83	31 (751)	0.03	1.7	357

c_{j-0} – the current degree of surface coverage with the polymer, calculated per molecule when the chain is positioned along the surface (before the layer begins to compress);

π_i–π_f, ($\Delta\pi$) – pressure range in which a stable state exists;

$A_{mol(link)}$ – area per link in nanostructures. The remaining parameters were calculated per molecule;

n_{link} the number of links in the nanostructure;

c_i– c_f – degrees of surface coverage at the initial and final points of the stable state;

D_{NS} and S_{NS} – diameter and area of nanostructures;

$w_{inter-M-i}$ – water content between M-nanostructures (per molecule) at the initial point of the stable state;

d_i – the distance between nanostructures at the point of the beginning of a stable state;
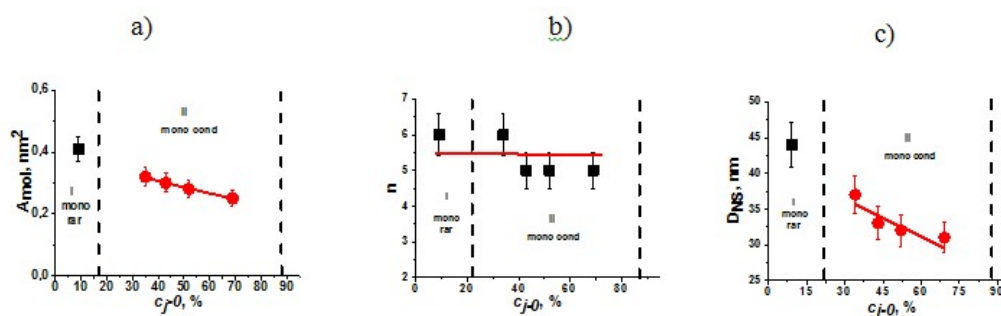
B – layer compressibility.

Figure 4. Dependences of: a) area per link in nanostructures; b) number of molecules in them; c) diameter of nanostructures on the current degree of surface coverage before the layer begins to compress.

monolayer condensed state is c_{bord_cond} = 93%, and taking into account the error in determining this value (5%) c_{bord_cond} = 88%. The minimum diameter of the formed nanostructures is (D_{NS}-min) 24 nm.

Thus, at different initial degrees of surface coverage at the water-air interface, the formation of two types of P4VP M-monolayers is possible. The conditions for the formation of rarefied (rar) and condensed (cond) monolayers were determined as follows: cj-0 ≤ 9% and 35 ≤ cj-0 ≤ 69%, respectively. Condensed monolayers, in contrast to rarefied ones, are characterized by smaller values of the area per molecule in them.

It has been established that the number of molecules in the nanostructure of a P4VP monolayer, regardless of the type of monolayer, is constant and does not depend on the initial degree of surface coverage and amounts to 5–6 polymer molecules in the nanostructure. Thus, the polymer in solution in the form of balls, when applied to the surface of water, can unfold and be located along the water-air interface.

Coordination of poly-4-vinylpyridine by CoTpMPP in layers on the surface of water

To carry out the coordination reaction, solutions in chloroform P4VP (C=1.12·10^{-7} M) and CoTpMPP (C=6.3·10^{-5} M) were sequentially applied to the water surface at a temperature of 21±1 °C. Component ratio: one porphyrin per 30 polymer units. The resulting layer was compressed to the appropriate pressure. Layer compression isotherms are shown in Figure 5. By transferring the layers onto a quartz plate, LS films were obtained. LS films were obtained under two different conditions. The first sample is at a surface pressure π = 4 mN/m (by transferring monolayers to the substrate, point A in Figure 5), the number of immersions of the substrate into the layer K = 23 (linear section of the isotherm). The second sample is a LS film formed at a surface pressure π = 53 mN/m (multilayers, number of substrate immersions into the layer K=7 (transfer conditions are shown by point B on the isotherms, Figure 5).

UV-Vis spectra of the resulting LS films are shown in Figure 6. The position of a very weak Soret band in the spectrum of the film obtained at low surface pressure (439 nm) is the same as in the spectrum of the LS film of the individual component – CoTpMPP (438–439 nm), which indicates the presence in the film there is a very small amount of CoTpMPP nanostructures (Figure 6a). The estimated content of porphyrin nanostructures under these conditions is about 5%. The second, main Soret band in the spectrum (430 nm, blue line and inset in Figure 6a) indicates the formation of a porphyrin polymer (P4VP + CoTpMPP). The layer on water consists of three components: a small amount of unreacted polymer (257 nm), a porphyrin polymer obtained as a result of the reaction (430 nm) and a small amount of CoTpMPP nanostructures (439 nm).
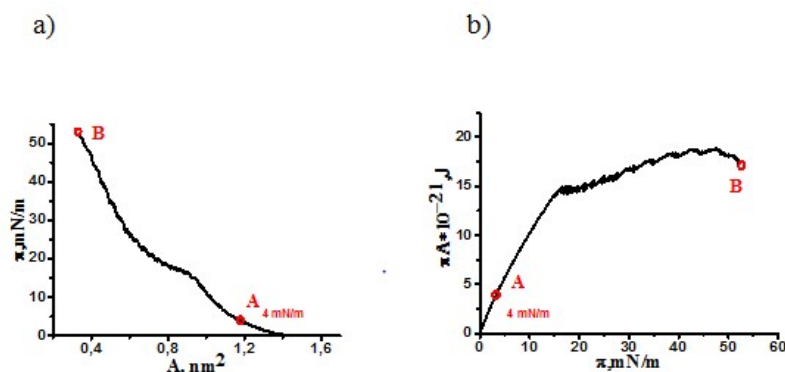

Figure 5. a) π–A, and b) πA–π isotherms of the polymer with porphyrin layer. Points A and B show the conditions for transferring layers to solid supports.
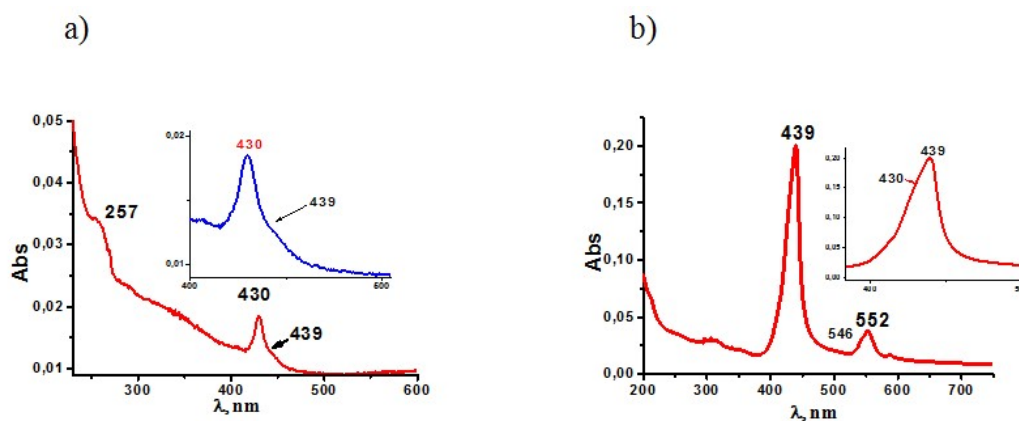

Figure 6. a) UV-Vis spectrum of the LS film of P4VP+CoTpMPP, state of the layer when transferred to the substrate – monolayer, K=23; b) UV-Vis spectrum of the LS film of P4VP+CoTpMPP, state of the layer when transferred to the substrate – multilayer, K=7.

In the UV-Vis spectrum of the film obtained by transferring multilayers (at high surface pressure, Figure 6b), a band corresponding to the porphyrin polymer (430 nm) is observed, as well as a band of similar intensity at 439 nm, which corresponds to CoTpMPP nanostructures. Note, that the position of the Q band in the spectrum of the CoTpMPP LS film is 550 nm, and in the spectrum of the P4VP-CoTpMPP porphyrin polymer film, obtained as a result of the reaction on the surface of water – 546 nm. It can be also assumed that in this case the porphyrin bound to the porphyrin polymer forms its own stacks on the surface of the water.

Conclusions

Nanostructured monolayers of poly-4-vinylpyridine at the water-air interface were obtained. It was found that the formation of two types of P4VP M-monolayers at different initial degrees of surface coverage (cj-0) on the water surface, is possible. The conditions for the formation of rarefied (rar) and condensed (cond) monolayers were determined as follows: cj-0 $\leq$ 9% and $35 \leq$ cj-0 $\leq$ 69%, respectively. Quantitative characteristics of their structure and properties are determined. A model of condensed monolayer was constructed and constants that were independent of the layer formation conditions were determined. It has been shown that a specific feature of P4VP monolayers is the independence of the number of molecules in the nanostructure of both types of P4VP monolayers on the initial degree of surface coverage in a wide range of values of this value (9–69%). This number is 5–6 polymer molecules in a nanostructure.

For the first time, by the coordination reaction of poly-4-vinylpyridine with cobalt tetra(*p*-methoxyphenyl)porphyrinate (CoTpMPP) in nanostructured layers at the water-air interface, the porphyrin polymer P4VP-CoTpMPP was obtained and studied in Langmuir-Schaefer films. The estimated content of porphyrin nanostructures in films obtained from layers formed at low surface pressure is only about 5%.

References

1. Sorokin A.B. *Chem. Rev.* **2013**, *113*, 8152
2. Yang S., Yu Y., Gao X., Zhang Z., Wang F. *Chem. Soc. Rev.* **2021**, *50*, 12985.
3. Demir E., Silah H., Uslu B. *Crit. Rev. Anal. Chem.* **2022**, *52*, 425.
4. De la Torre G., Bottari G., Torres T. *Adv. Energy Mater.* **2017**, *7*, 1601700.
5. Battersby A.R. *Nat. Prod. Rep.* **2000**, *17*, 507–526.
6. Warren M.J. *Tetrapyrroles: Birth, Life and Death.* Springer Science & Business Media. **2009**, 406 p.
7. Keely B.J. Geochemistry of Chlorophylls. In: *Chlorophylls and Bacteriochlorophylls. Advances in Photosynthesis and Respiration, Vol. 25* (Grimm B., Porra R.J., Rüdiger W., Scheer H., Eds.) Springer, Dordrecht, **2006**, p. 535–561.
8. Wojaczynski J., Latos-Grażyński L. *Coord. Chem. Rev.* **2000**, *204*, 113–171.
9. Valkova L., Borovkov N., Pisani M., Rustichelli F. *Thin Solid Films* **2001**, *401*, 267.
10. Petrova M.V., Maiorova L.A., Bulkina T.A., Ageeva T.A., Koifman O.I., Gromova O.A. *Macroheterocycles* **2014**, *7*, 267–271.
11. Valkova L., Borovkov N., Kopranenkov V., Pisani M., Bossi M., Rustichelli F. *J. Mater. Sci. Eng. C* **2002**, *22*, 167.
12. Zhang Z., Wojtas L., Zaworotko M.J. *Cryst. Growth Des.* **2014**, *14*, 1526.
13. Bo Q., Zhao Y. *J. Polym. Sci. Pol. Chem.* **2006**, *44*, 1734.
14. Tagliatesta P., Carbone M. *Encapsulated Catalysts* **2017**, 249–278.
15. Managa M., Nyokong T. *Macroheterocycles* **2017**, *10*, 467.
16. Zhang Z., Zhang L., Wojtas L., Nugent P., Eddaoudi M., Zaworotko M.J. *J. Am. Chem. Soc.* **2012**, *134*, 924.
17. Wohrle D., Pomogailo A.D. *Metal Complexes and Metals in Macromolecules.* Wiley-VCH. Weinheim, **2003**. 667 p.
18. Wark M. Porphyrins and Phthalocyanines Encapsulated in Inorganic Host Materials. In: *The Porphyrin Handbook, Vol. 17.* **2003**, p. 247–283.
19. Sanders J.K.M., Bampos N., Clyde-Watson Z., Darling S.L., Hawley J.C., Kim H.-J., Mak C.C., Webb S.J. Axial Coordination Chemistry of Metalloporphyrins. In: *The Porphyrin Handbook, Vol. 3.* **2000**, p. 48.
20. Valkova L., Menelle A., Borovkov N., Erokhin V., Pisani M., Ciuchi F., Carsughi F., Spinozzi F., Pergolini M., Padke R., Bernstorff S., Rustichelli F. *J. Appl. Cryst.* **2003**, *36*, 758–762.
21. Valkova L.A., Shabyshev L.S., Borovkov N.Y., Feigin L.A., Rustichelli F. *J. Incl. Phenom. Macrocycl. Chem.* **1999**, *35*, 243.
22. Maiorova L.A., Koifman O.I., Burmistrov V.A., Kuvshinova S.A., Mamontov A.O. *Prot. Met. Phys. Chem. Surf.* **2015**, *51*, 85.
23. Valkova L.A., Shabyshev L.S., Feigin L.A., Akopova O.B. *Izv. Akad. Nauk Fiz.* **1997**, *61*, 631.
24. Shin J., Kim J., Park S.H., Ha T.X. *ACS Nano* **2018**, *12*, 9423.
25. Zhang T.D., Deng X., Wang X., Chen M.Y., Wang L.L., Li X.T., Shi C.Y., Lin W.P., Li W.U., Pan Q., Ni W., Pan X., Yin T., Yin D.C. *ACS Appl. Mater. Interfaces.* **2021**, *13*, 46391−46405.
26. Xiong R., Kim H.Sh., Zhang Sh., Kim S., Korolovych V.F., Ma R., Yingling Y.G., Lu C., Tsukruk V.V. *ACS Nano* **2017**, *11*, 12008−12019.
27. Rubia-Payá C., de Miguel G., Martín-Romero M.T., Giner-Casares J.J., Camacho L. *Adv. Colloid Interfac. Sci.* **2015**, *225*, 134.
28. Valkova L.A., Shabyshev L.S., Feigin L.A., Akopova O.B. *Mol. Cryst. Liq. Cryst. Sci. Tech. C* **1996**, *6*, 291.
29. Valkova L.A., Betrencourt C., Hochapfel A., Myagkov I.V., Feigin L.A. *Mol. Cryst. Liq. Cryst. Sci. Tech. A* **1996**, *287*, 269.
30. Yamamoto S., Nagatani H., Imura H. *Langmuir* **2017**, *33*, 10134.
31. Kuzmin S.M., Chulovskaya S.A., Parfenyuk V.I. *Electrochim. Acta* **2020**, *342*, 136064.
32. Kuzmin S.M., Chulovskaya S.A., Parfenyuk V.I. *Electrochim. Acta* **2018**, *292*, 256.
33. Mon M., Bruno R., Ferrando-Soria J., Armentano D., Pardo E. *J. Mater. Chem. A* **2018**, *6*, 4912−4947.
34. Li D.-J., Li Q.-H., Gu Z.-G., Zhang J. *Nano Lett.* **2021**, *21*, 10012−10018.
35. Ariga K., Nishikawa M., Mori T., Takeya J., Shrestha L.K., Hill J.P. *Sci. Technol. Adv. Mater.* **2019**, *20*, 51–95.

36. Webre W.A., Gobeze H.B., Shao S., Karr P.A., Ariga K., Hill J.P., D'Souza F. *Chem. Commun.* **2018**, *54*, 1351–1354.

37. Topchieva I.N., Osipova S.V., Banatskaya M.I., Valkova L.A. *Dokl. Akad. Nauk SSSR* **1989**, *308*, 910–913.

38. Valkova L.A., Glibin A.S., Valli L. *Colloid J.* **2008**, *70*, 6–11.

39. Oldacre A.N., Friedman A.E., Cook T.R. *J. Am. Chem. Soc.* **2017**, *139*, 1424−1427.

40. Brenner W., Ronson T.K., Nitschke J.R. *J. Am. Chem. Soc.* **2017**, *139*, 75–78.

41. Valkova L.A., Erokhin V.V., Glibin A.S., Koifman O.I. *J. Porphyrins Phthalocyanines* **2011**, *15*, 1044–1051.

42. Ariga K., Mori T., Nakanishi W., Hill J.P. *Phys. Chem. Chem. Phys.* **2017**, *19*, 23658–23676.

43. Ariga K., Tsai K.C., Shrestha L.K., Hsu S.H. *Mater. Chem. Front.* **2021**, *5*, 1018–1032.

44. Huang Z., Qin B., Chen L., Xu J.F., Faul C.F., Zhang X. *Macromol. Rapid Commun.* **2017**, *38*, 1700312−1700326.

45. Yang L., Tan X., Wang Z., Zhang X. *Chem. Rev.* **2015**, *115*, 7196−7239.

46. Shee N.K., Kim M.K., Kim H.J. *Nanomaterials* **2020**, *10*, 2314–2329.

47. Huo Z., Lates V., Ibrahim H., Goldmann M., Xu H., Yi T. *Eur. J. Org. Chem.* **2021**, *2021*, 6636−6645.

48. Stulz E. *Acc. Chem. Res.* **2017**, *50*, 823−831.

49. Maiorova L.A., Kobayashi N., Zyablov S.V., Bykov V.A., Nesterov S.I., Kozlov A.V. *Langmuir* **2018**, *34*, 9322−9329.

50. Kharitonova N.V., Maiorova L.A., Koifman O.I. *J. Porphyrins Phthalocyanines* **2018**, *22*, 509−512.

51. Vu T.T., Maiorova L.A., Berezin D.B., Koifman O.I. *Macroheterocycles* **2016**, *9*, 73–79.

52. Karlyuk M.V., Krygin Y.Y., Maiorova L.A., Ageeva T.A., Koifman O.I. *Russ. Chem. Bull.* **2013**, *62*, 471–479.

53. Maiorova L.A., Kobayashi N., Salnikov D.S., Kuzmin S.M., Basova T.V., Koifman O.I., Parfenyuk V.I., Bykov V.A., Bobrov Y.A., Yang P. *Langmuir* **2023**, *39*, 3246−3254.

54. Singh A., Samanta S., Kumar A., Debnath A.K., Prasad R., Veerender P., Balouria V., Aswal D.K., Gupta S.K. *Org. Electron.* **2012**, *13*, 2600–2604.

55. Sizuna T., Bouveta M., Chena Y., Suissea J.-M., Barochia G., Rossignol J. *Sens. Actuators B* **2011**, *159*, 163–170

56. Klyamer D.D., Sukhikh A.S., Krasnov P.O., Gromilov S.A., Morozova N.B., Basova T.V. *Appl. Surf. Sci.* **2016**, *372*, 79–86.

57. Klyamer D., Shao W., Krasnov P., Sukhikh A., Dorovskikh S., Popovetskiy P., Li X., Basova T. *Biosensors* **2023**, *13*, 484.

58. Bohrer F.I., Sharoni A., Colesniuc C., Park J., Schuller I.K., Kummel A.C., Trogler W.C. *J. Am. Chem. Soc.* **2007**, *129*, 5640–5646.

59. Koifman O.I., Ageeva T.A. *Porphyrin Polymers. Synthesis, Properties, Applications*, Moscow: URSS. **2018**, 300 p. [Койфман О.И., Агеева Т.А. *Порфиринполимеры: Синтез, свойства, применение*. URSS. **2018**. 300 с.] ISBN 978-5-9710-6121-2.

60. Esteves C.H.A., Iglesias B.A., Li R.W.C., Ogawa T., Gruber J. *Sensor. Actuat. B-Chem.* **2014**, *193*, 136–141.

61. Ribeiro S.M., Serra A.C., d'A Gonsalves Rocha A.M. *J. Mol. Catal. A-Chem.* **2010**, *326*, 121–127.

62. Ye Yu.-J., Zhou X.-T., Huang J.-W., Cai J.-H. *J. Mol. Catal. A-Chem.* **2010**, *331*, 29–34.

63. Lv Y-Y., Wu J., Xu Z-K. *Sensor. Actuat. B-Chem.* **2010**, *148*, 233–239.

64. Patel E.K., Oswal R.J. *IJRPC* **2012**, *2*(2), 237.

65. Chai Z., Jing Ch., Liu Y., An Y., Shi L. *Colloid Polym Sci.* **2014**, *292*, 1329–1337.

66. Niu X., Li N., Zhu Ch., Liu L., Zhao Y., Ge Y., Chen Y., Xu Z., Lu Y., Sui M., Li Y., Tarasov A., Goodilin E.A., Zhou H., Chen Q. *J. Mater. Chem. A* **2019**, *7*, 7338.

67. Nasirmahale L.N., Jolodar O.G., Shirini F., Tajik H. *Polycycl. Aromat. Comp.* **2019**, *41*, 199–210.

68. Shanmugam P., Wei E., Xie J., Murugan E. *Asian J. Chem.* **2019**, *31*, 235–246.